

Supporting Information

Organic light emitting diodes with horizontally oriented thermally activated delayed fluorescence emitters

Dae-Hyeon Kim^a, Ko Inada^a, Li Zhao^a, Takeshi Komino^{a,b,c}, Naoki Matsumoto^d, Jean-Charles Ribierre^{a,b,*}, Chihaya Adachi^{a,b,e*}

^aCenter for Organic Photonics and Electronics Research (OPERA), Kyushu University, 744 Motoooka, Nishi, Fukuoka 819-0395, Japan

^bJapan Science and Technology Agency (JST), ERATO, Adachi Molecular Exciton Engineering Project, c/o Center for Organic Photonics and Electronics Research (OPERA), Kyushu University, 744 Motoooka, Nishi, Fukuoka 819-0395, Japan

^cEducation Center for Global Leaders in Molecular System for Devices, Kyushu University, 744 Motoooka, Nishi, Fukuoka 819-0395, Japan

^dTosoh Corp., Nanyo Research Laboratory, 4560 Kaisei-cho, Shunan, Yamaguchi 746-8501, Japan

^eInternational Institute for Carbon Neutral Energy Research (WPI-I2CNER), Kyushu University, 744 Motoooka, Nishi, Fukuoka 819-0395, Japan

*Authors to whom correspondence should be addressed. Electronic addresses: ribierre@opera.kyushu-u.ac.jp and adachi@cstf.kyushu-u.ac.jp

Table of contents

S1 synthesis.

Figure S1. Molecular structures as viewed along the long axes. Carbazole moieties are colored red.

Figure S2. Absorption and steady-state photoluminescence (PL) spectra of the neat films.

Figure S3. Optical characteristic for singlet and triplet energy level by streak camera.

Figure S4. Transient photoluminescence decays in toluene solution.

Figure S5. Experimental and simulated ellipsometric data ψ and Δ at different angles of incidence.

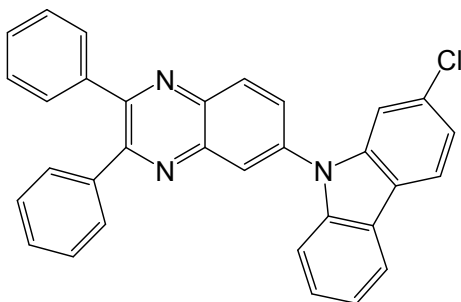
Figure S6. Calculated absorption spectra and oscillator strengths of the different electronic transitions.

Figure S7. 3D animations showing the optimized geometries of the TADF emitters and the directions of the absorption transition dipoles with a large oscillator strength.

Figure S8. J-V curves of hole-only devices to determine charge carrier mobilities using the SCLC method

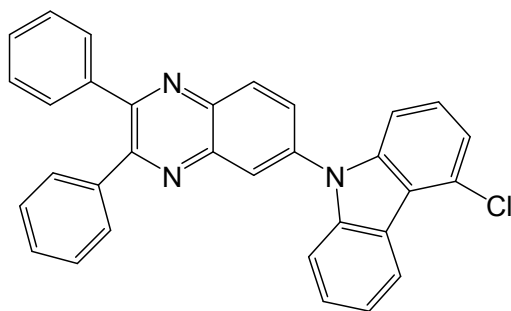
S1 synthesis of the compounds

The procedure to synthesize the four TADF luminophores developed in this study is explained below. ^1H NMR and ^{13}C NMR spectra were recorded with a Varian Gemini 200 (200 MHz) spectrometer. Chemical shifts of ^1H and ^{13}C NMR signals are in parts per million relative to tetramethylsilane as internal standard.



A threenecked flask was charged with 2-chlorocarbazole (0.60 g, 3.00 mmol), 6-bromo-2,3-diphenylquinoxaline (1.08 g, 3.00 mmol), K_2CO_3 (0.62 g, 4.50 mmol), $\text{Pd}(\text{OAc})_2$ (0.006 g, 0.030 mmol), P^tBu_3 (0.021 g, 0.105 mmol) and *o*-xylene (10 ml) under a nitrogen atmosphere. The reaction mixture was heated at 130°C for 8 h, and then cooled to room temperature. To the reaction mixture was added water (10 mL), extracted by tetrahydrofuran for two times, dried over MgSO_4 , and evaporated in vacuum to afford the crude product, which was further purified by column chromatography on silica gel with *n*-hexane/toluene to give 2-chloro-9-(2,3-diphenylquinoxaline-6-yl)carbazole (1.20g, 2.49mmol, 83%) as a yellow solid.

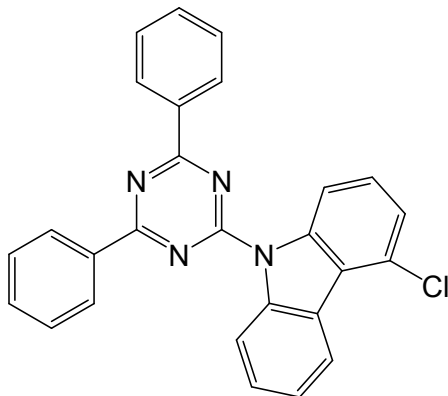
^1H NMR (CDCl_3 , 200 MHz) δ 8.36-8.39 (m, 2H), 8.02-8.11(m, 2H), 7.94 (d, 1H), 7.27-7.55 (m, 15H); ^{13}C NMR (CDCl_3 , 200 MHz) δ 154.81, 154.32, 142.20, 141.30, 141.10, 140.53, 139.08, 139.02, 138.64, 132.36, 131.45, 130.17, 129.45, 129.38, 129.00, 128.67, 126.83, 126.21, 123.53, 122.70, 121.59, 121.44, 121.38, 120.72, 110.27



A threenecked flask was charged with 4-chlorocarbazole (0.60 g, 3.00 mmol), 6-bromo-2,3-diphenylquinoxaline (1.08 g, 3.00 mmol), K_2CO_3 (0.62 g, 4.50 mmol), $\text{Pd}(\text{OAc})_2$ (0.006 g, 0.030 mmol), P^tBu_3 (0.021 g, 0.105 mmol) and *o*-xylene (10 ml) under a nitrogen atmosphere. The reaction mixture was heated at 130°C for 8 h, and then cooled to room temperature. To the reaction mixture was added water (10 mL), extracted by tetrahydrofuran for two times, dried over MgSO_4 , and evaporated in vacuum to afford the crude product, which was further purified by column chromatography on silica gel with *n*-hexane/toluene to

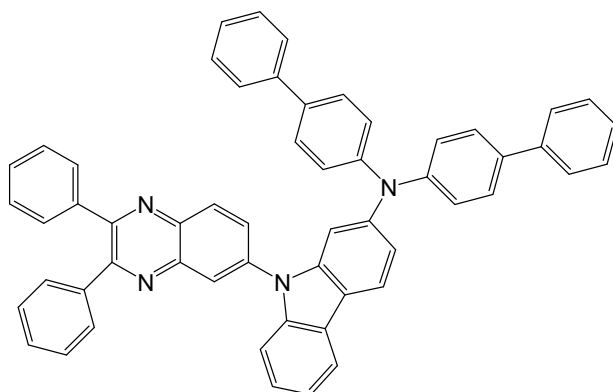
give 4-chloro-9-(2,3-diphenylquinoxaline-6-yl)carbazole (1.31g, 2.72mmol, 90%) as a yellow solid.

^1H NMR (CDCl_3 , 200 MHz) δ 8.70 (d, 1H), 8.35-8.38 (m, 2H), 7.92 (d, 1H), 7.28-7.56 (m, 16H); ^{13}C NMR (CDCl_3 , 200 MHz) δ 154.77, 154.35, 142.15, 141.93, 140.96, 140.59, 139.08, 139.02, 138.72, 131.36, 130.17, 129.46, 129.40, 129.33, 129.28, 128.68, 127.07, 126.70, 123.62, 123.03, 121.74, 121.35, 121.27, 109.89, 108.46



NaH (60% dispersion in mineral oil, 1.43 g, 35.75 mmol) was added in portions at 0°C to a stirred solution of 4-chlorocarbazole (6.00 g, 29.84 mmol) in DMF (30 mL). After stirring for 30 min at 0°C , 2-chloro-4,6-diphenyl-1,3,5-triazine (7.95 g, 28.08 mmol) was added and the mixture was stirred at room temperature for 1 h. The reaction mixture was poured into water (500 mL) and the precipitate was collected by filtration. Then, obtained solid was washed with water and methanol and is dried under vacuum to give 4-chloro-9-(4,6-diphenyl-1,3,5-triazine-2-yl)carbazole (9.44 g, 21.84mmol, 73%) as a pale yellow solid.

^1H NMR (CDCl_3 , 200 MHz) δ 9.13 (d, 1H), 9.07 (d, 1H), 8.71-8.73 (m, 5H), 7.59-7.66 (m, 7H), 7.39-7.50 (m, 3H); ^{13}C NMR (CDCl_3 , 200 MHz) δ 172.51, 165.10, 140.32, 139.18, 136.00, 132.85, 129.12, 128.83, 128.35, 127.38, 126.96, 125.33, 124.32, 123.56, 123.32, 122.93

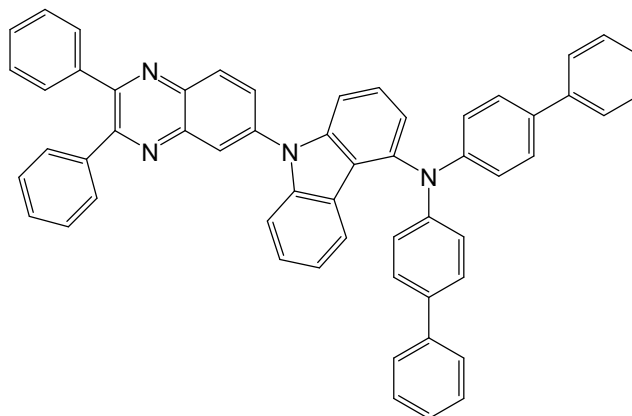


BDQC-2

A threenecked flask was charged with 2-chloro-9-(2,3-diphenylquinoxaline-6-yl)carbazole (1.00 g, 2.07 mmol), *N,N*-bis(1,1'-biphenyl-4-yl)amine (0.665 g, 2.07 mmol), NaO^tBu (0.278 g, 2.89 mmol), Pd(OAc)₂ (0.004 g, 0.020 mmol), P^tBu₃ (0.014 g, 0.070 mmol) and *o*-xylene (10 ml) under a nitrogen atmosphere. The reaction mixture was heated at 130°C for 8 h, and then cooled to room temperature. To the reaction mixture was added water (10 mL), extracted

by tetrahydrofuran for three times, dried over MgSO₄, and evaporated in vacuum to afford the crude product, which was further purified by column chromatography on silica gel with *n*-hexane/toluene to give Cz7 (1.44g, 1.88mmol, 91%) as a yellow solid.

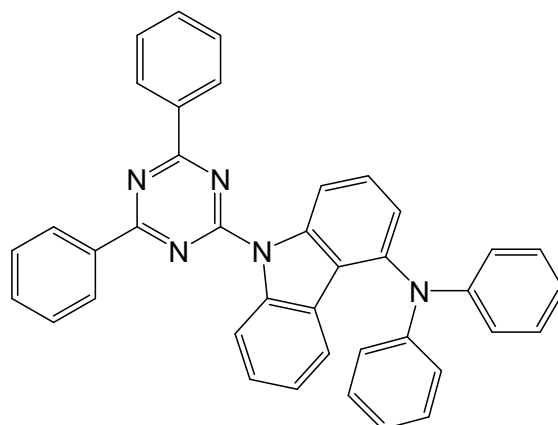
¹H NMR (CDCl₃, 200 MHz) δ 8.24-8.33 (m, 2H), 8.02-8.06 (m, 2H), 7.90 (d, 1H), 7.13-7.54 (m, 33H); ¹³C NMR (CDCl₃, 200 MHz) δ 154.63, 154.07, 147.54, 146.67, 142.25, 141.84, 141.33, 140.85, 140.43, 139.15, 139.06, 135.44, 131.25, 130.14, 129.31, 129.26, 129.14, 129.06, 128.61, 128.08, 127.11, 126.91, 126.08, 125.97, 124.20, 124.11, 121.58, 121.22, 120.38, 120.28, 119.55, 110.01, 106.74



BDQC-4

A threenecked flask was charged with 4-chloro-9-(2,3-diphenylquinoxaline-6-yl)carbazole (1.00 g, 2.07 mmol), *N,N*-bis(1,1'-biphenyl-4-yl)amine (0.665 g, 2.07 mmol), NaO^tBu (0.278 g, 2.89 mmol), Pd(OAc)₂ (0.004 g, 0.020 mmol), P^tBu₃ (0.014 g, 0.070 mmol) and *o*-xylene (10 ml) under a nitrogen atmosphere. The reaction mixture was heated at 130°C for 8 h, and then cooled to room temperature. To the reaction mixture was added water (10 mL), extracted by tetrahydrofuran for three times, dried over MgSO₄, and evaporated in vacuum to afford the crude product, which was further purified by column chromatography on silica gel with *n*-hexane/toluene to give Cz4-2 (1.37g, 1.78mmol, 86%) as a yellow solid.

¹H NMR (CDCl₃, 200 MHz) δ 8.24-8.33 (m, 2H), 8.39-8.47 (m, 2H), 8.04 (d, 1H), 7.92 (d, 1H), 7.22-7.56 (m, 32H), 7.06-7.16 (m, 2H); ¹³C NMR (CDCl₃, 200 MHz) δ 154.72, 154.23, 146.96, 142.64, 142.25, 141.49, 140.97, 140.79, 140.52, 139.12, 139.08, 134.90, 131.23, 130.16, 129.52, 129.42, 129.35, 128.99, 128.67, 128.13, 127.53, 126.97, 126.88, 126.58, 126.44, 123.59, 122.33, 121.49, 121.22, 109.61, 107.88



DTDC

A threenecked flask was charged with 4-chloro-9-(4,6-diphenyl-1,3,5-triazine-2-yl)carbazole (1.30 g, 3.01 mmol), *N,N*-diphenylamine (0.535 g, 3.15 mmol), NaO^tBu (0.404 g, 4.21 mmol), Pd(OAc)₂ (0.006 g, 0.030 mmol), P^tBu₃ (0.021 g, 0.105 mmol) and *o*-xylene (10 ml) under a nitrogen atmosphere. The reaction mixture was heated at 130°C for 8 h, and then cooled to room temperature. The precipitate was collected by filtration and was washed with water and methanol. The crude solid was recrystallized from *o*-xylene to give Cz4-3 (1.46g, 2.58mmol, 85%) as a white solid.

¹H NMR (CDCl₃, 200 MHz) δ 9.06 (d, 2H), 8.75 (d, 4H), 7.96 (d, 1H), 7.56-7.67 (m, 7H), 7.50 (t, 1H), 7.12-7.24 (m, 10H), 6.92-6.97 (m, 2H); ¹³C NMR (CDCl₃, 200 MHz) δ 172.78, 165.38, 147.65, 141.26, 141.11, 139.28, 136.41, 133.07, 129.49, 129.40, 129.11, 128.15, 127.08, 125.21, 125.05, 124.37, 123.67, 123.01, 122.23, 121.94, 116.92, 115.22

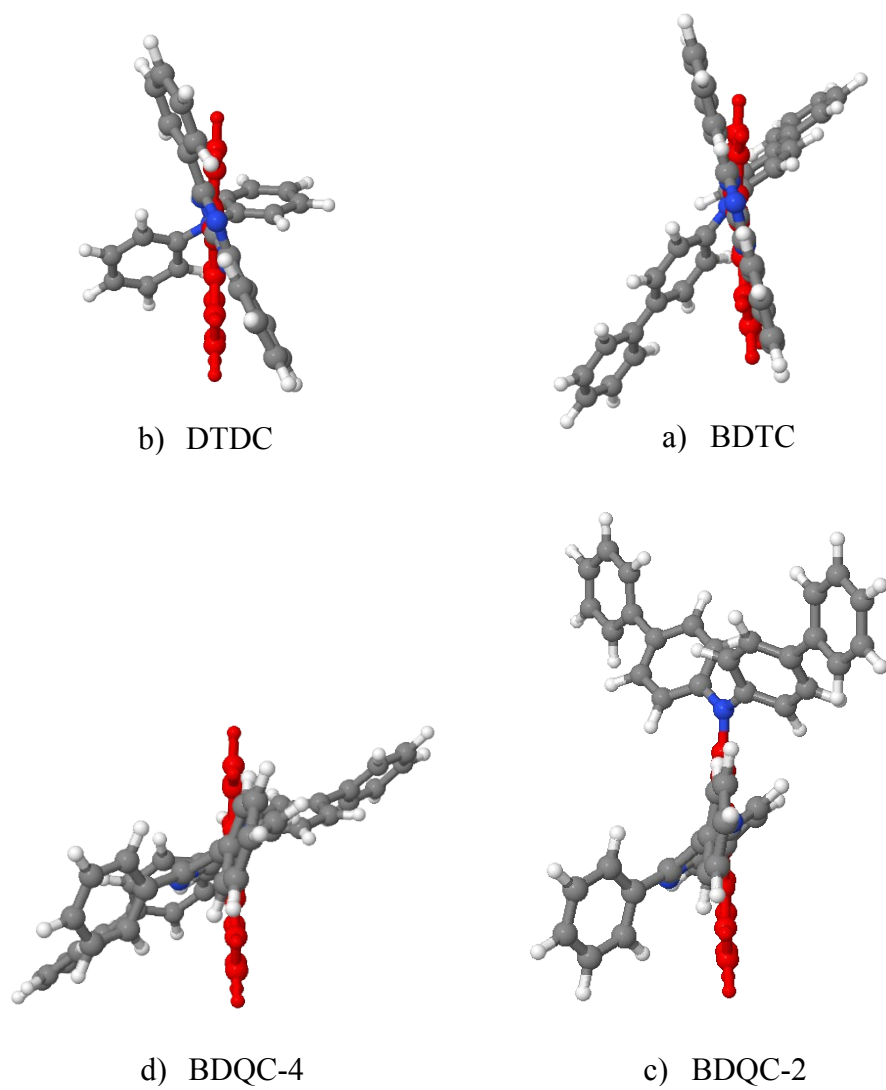


Figure S1. Molecular structures of a) DTDC, b) BDTC, c) BDQC-4 and d) BDQC-2 as viewed along the long axes. Carbazole moieties are colored red.

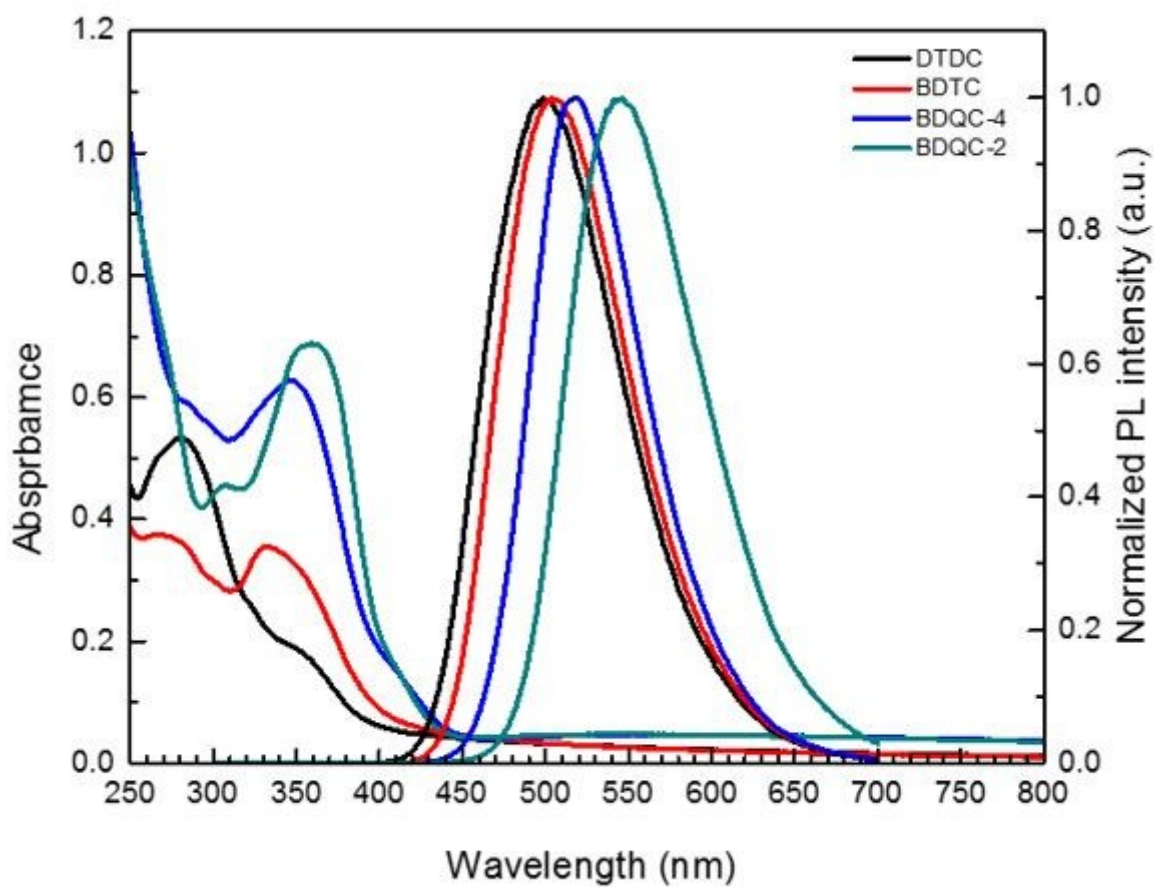


Figure S2. Absorption (left) and normalized steady-state fluorescence (right) spectra of the TADF luminophores in neat films. These spectra were measured at room temperature. Excitation wavelength for the PL spectra was 499, 505, 517 and 546 nm.

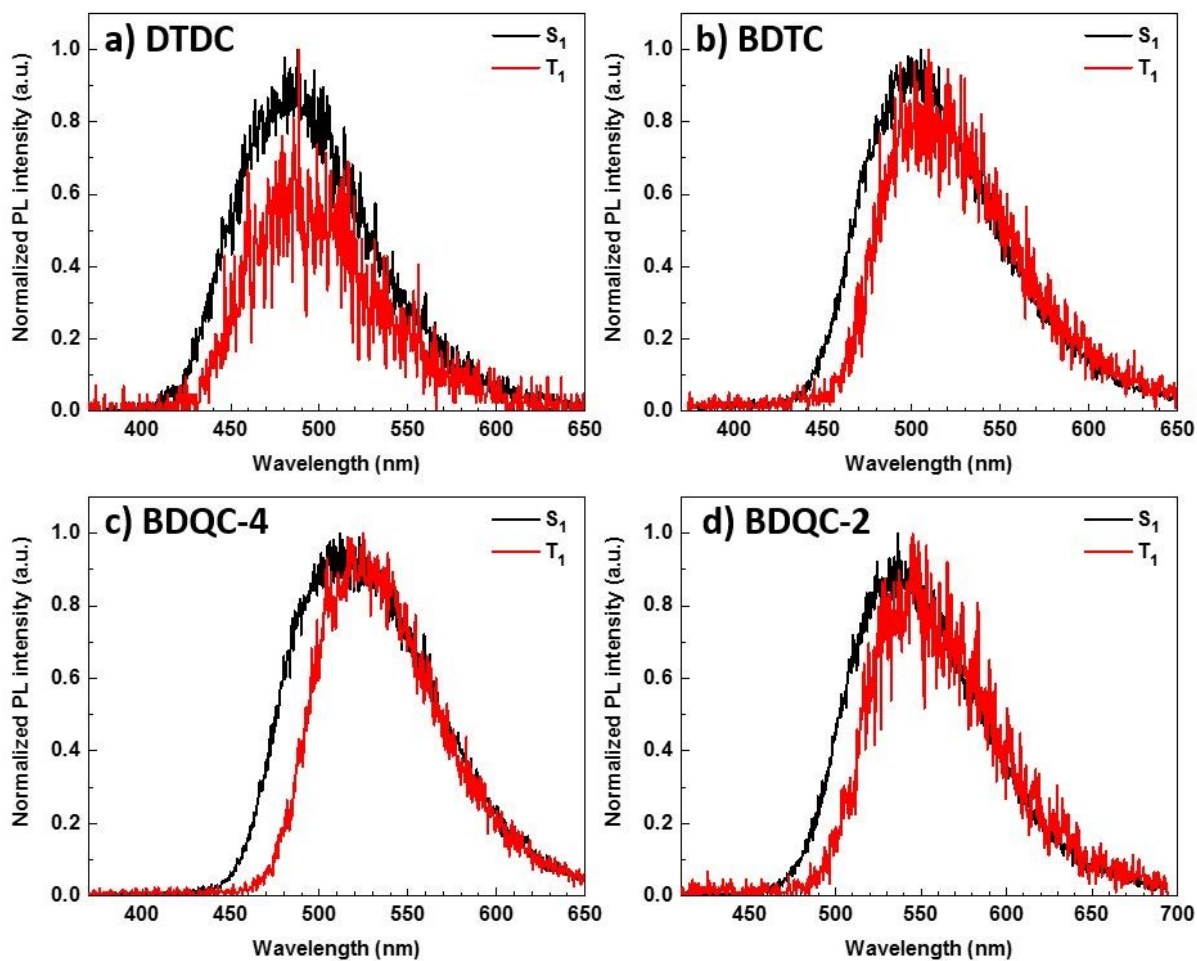


Figure S3. Photoluminescence spectra of a) DTDC, b) BDTC, c) BDQC-4 and d) BDQC-2 neat films recorded with a streak camera. Fluorescence and phosphorescence spectrums were recorded at 5 K. Excitation wavelength was 337 nm (from a pulsed nitrogen laser).

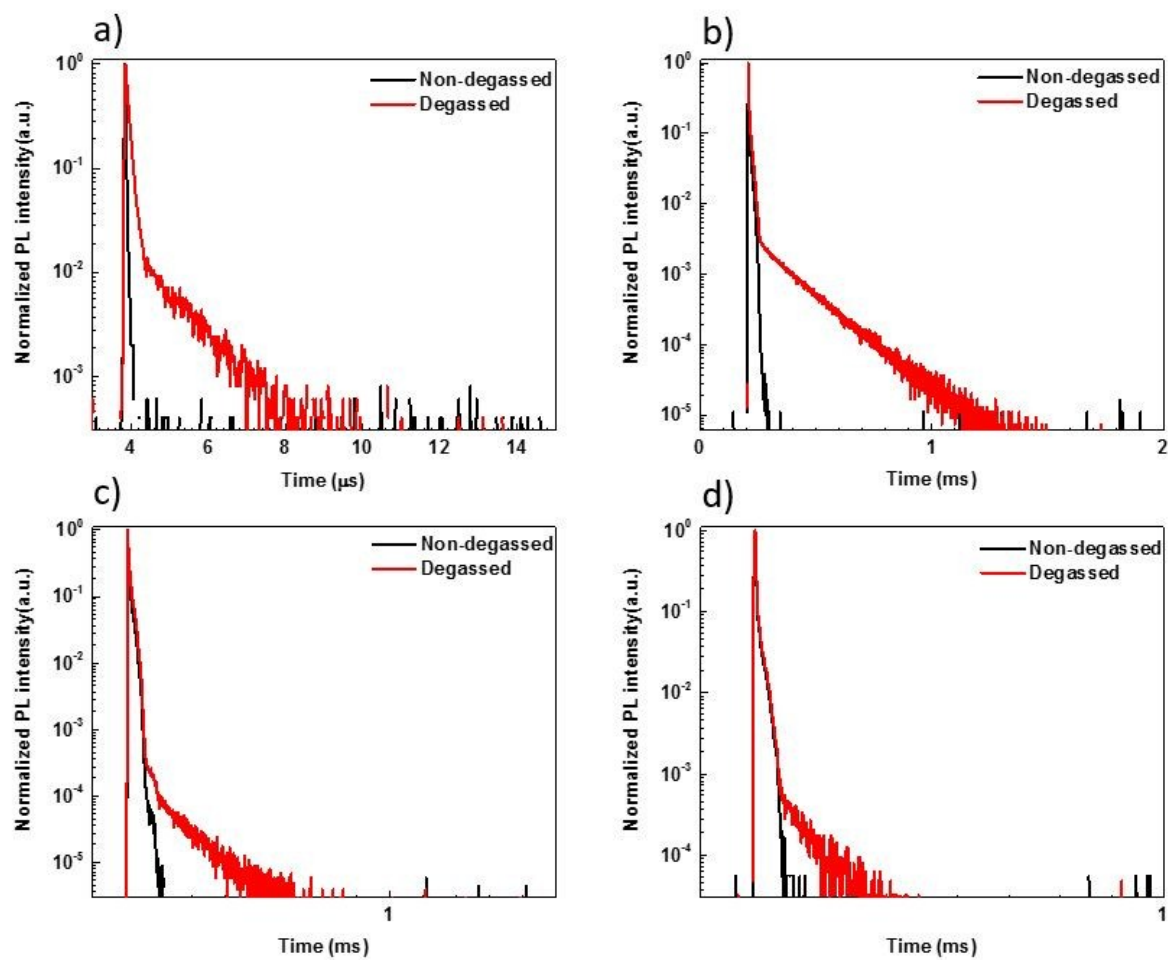


Figure S4. Transient photoluminescence decay curves for (a) DTDC, (b) BDTc, (c) BDQC-4 and (d) BDQC-2 in degassed and non-degassed toluene solutions. Excitation wavelength was 337 nm.

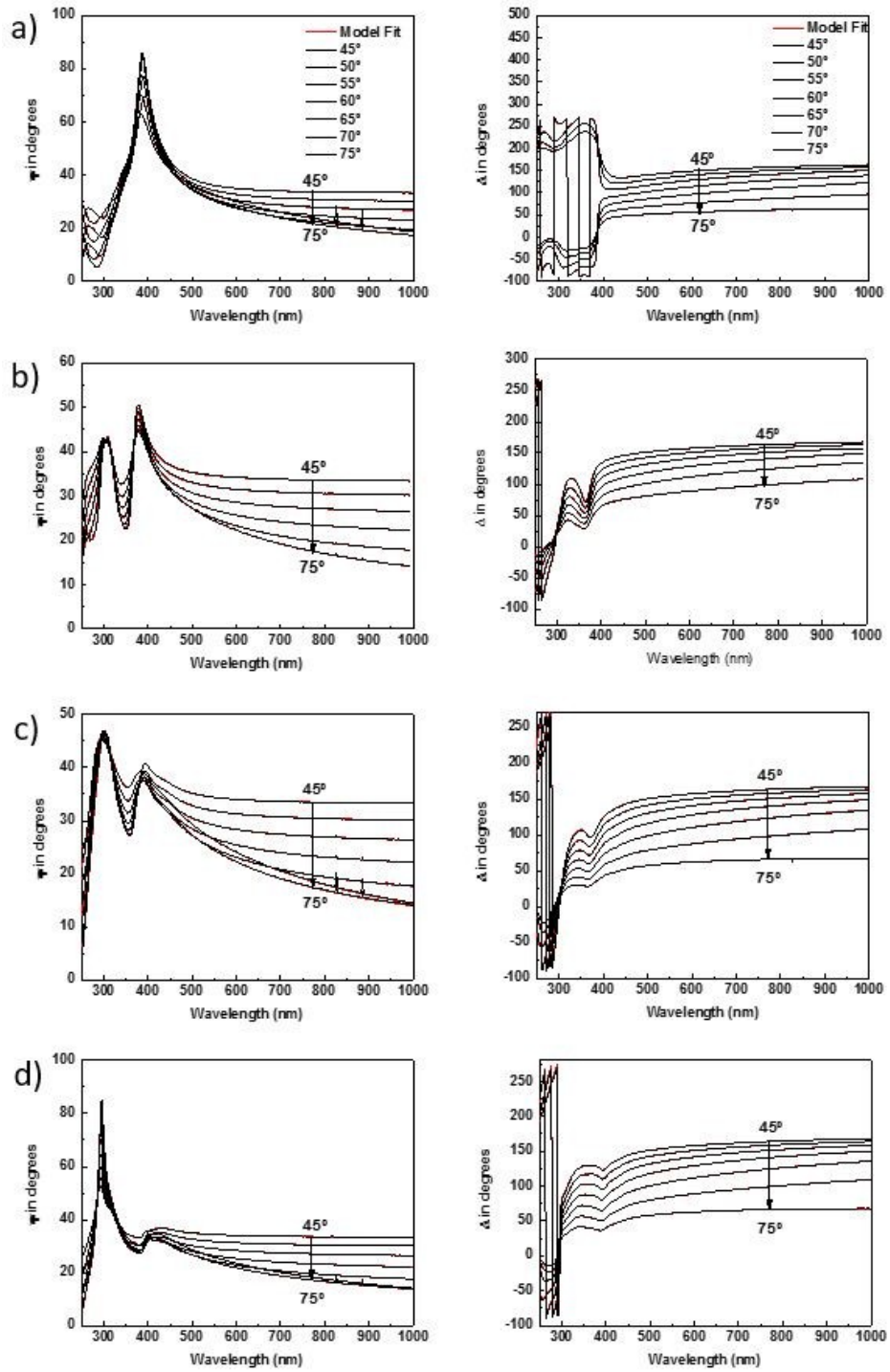


Figure S5. Experimental and simulated ellipsometric data ψ and Δ at different angles of incidence in a) DTDC, b) BDTC c) BDQC-4 and d) BDQC-2 neat films.

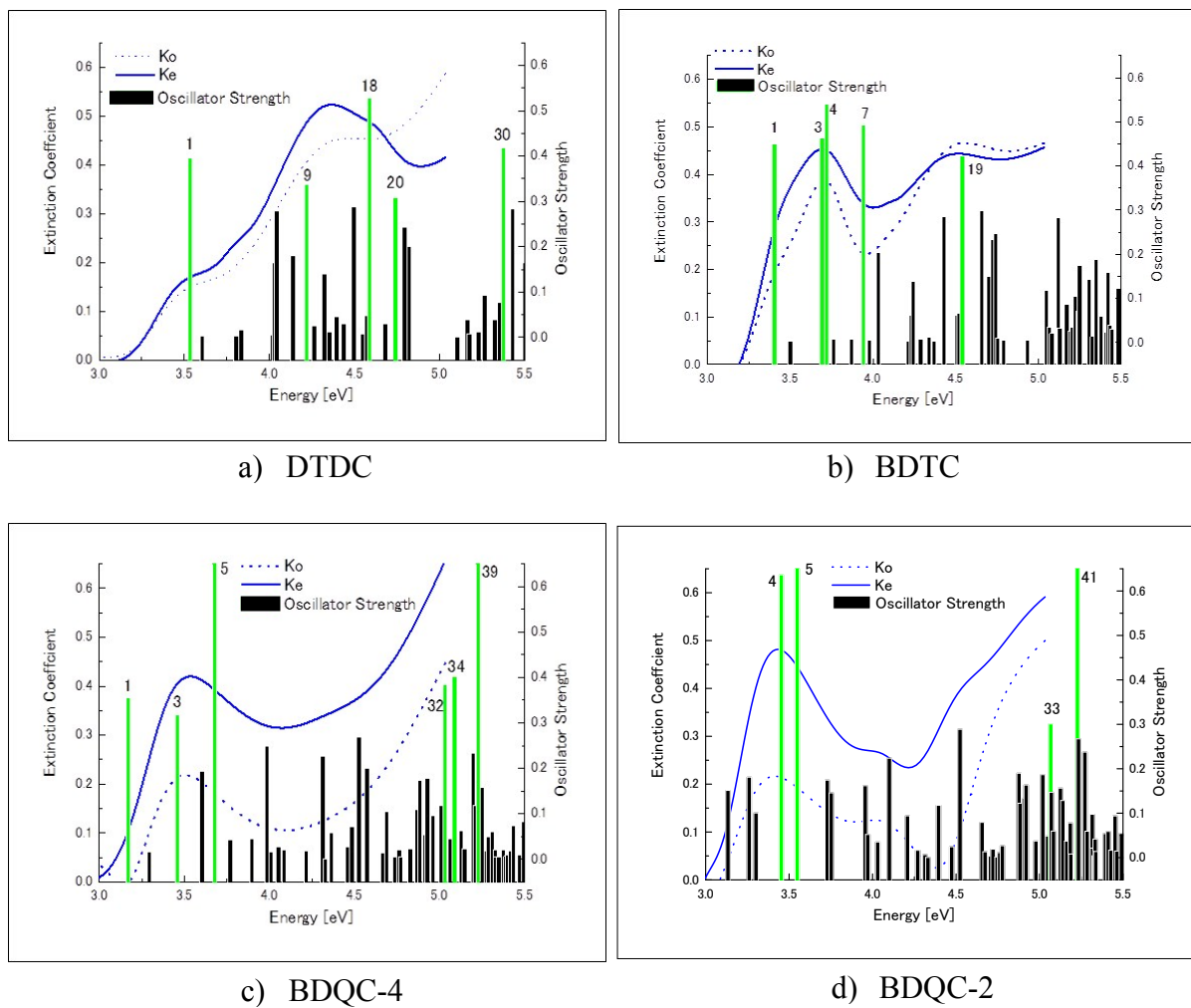


Figure S6. Calculated oscillator strengths of the TADF emitters at the LC-wPBE*/6-31+G(d) level with the measured extinction coefficients. Oscillator strengths higher than 0.3 eV are highlighted by green, and numbers indicate the corresponding excited states.

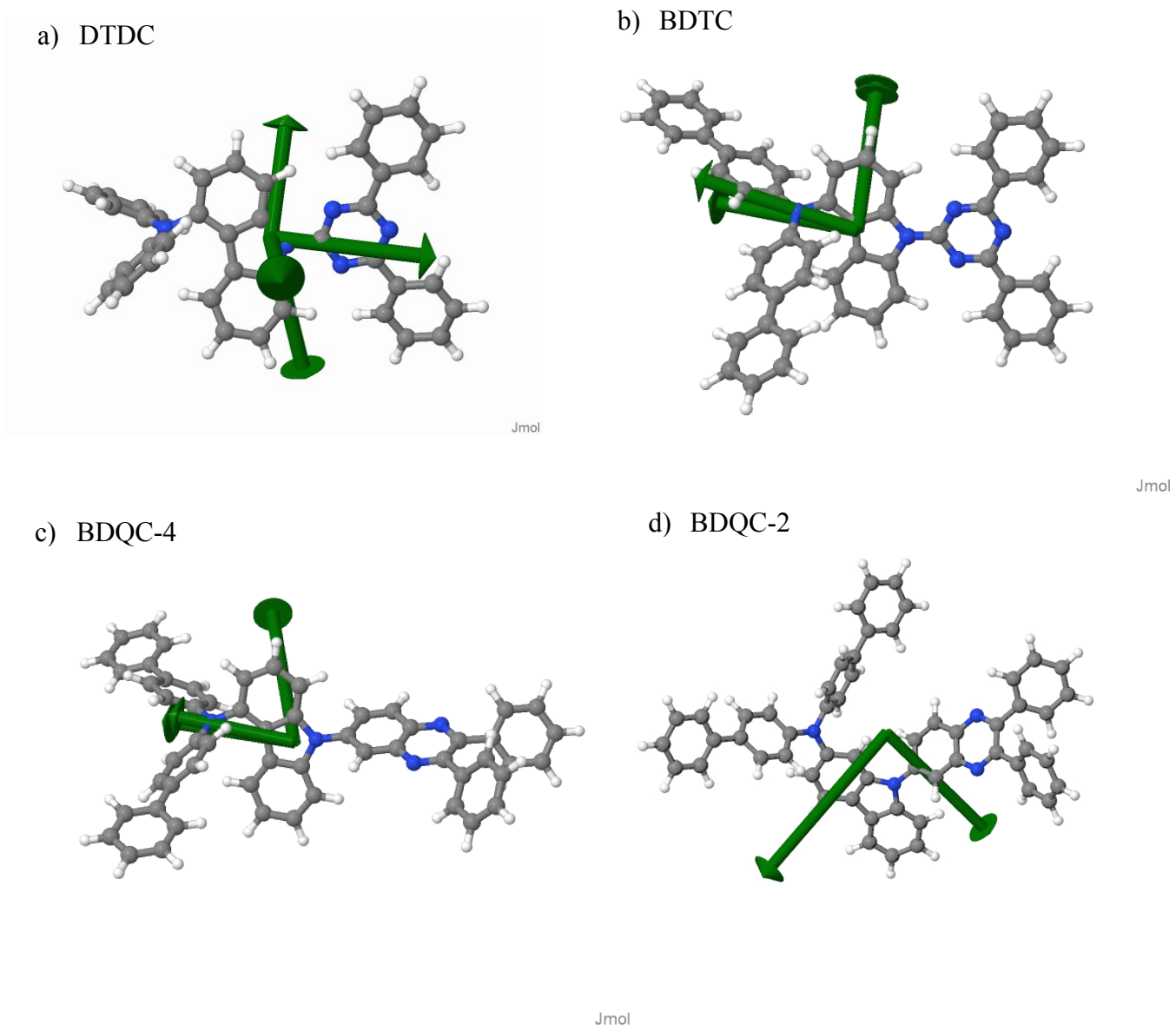


Figure S7. 3D animations showing the optimized ground state geometries of the four TADF emitters and the directions of the absorption transition dipoles from the lowest energy extinction coefficient peaks in Figure S6 with oscillator strengths higher than 0.3 eV.

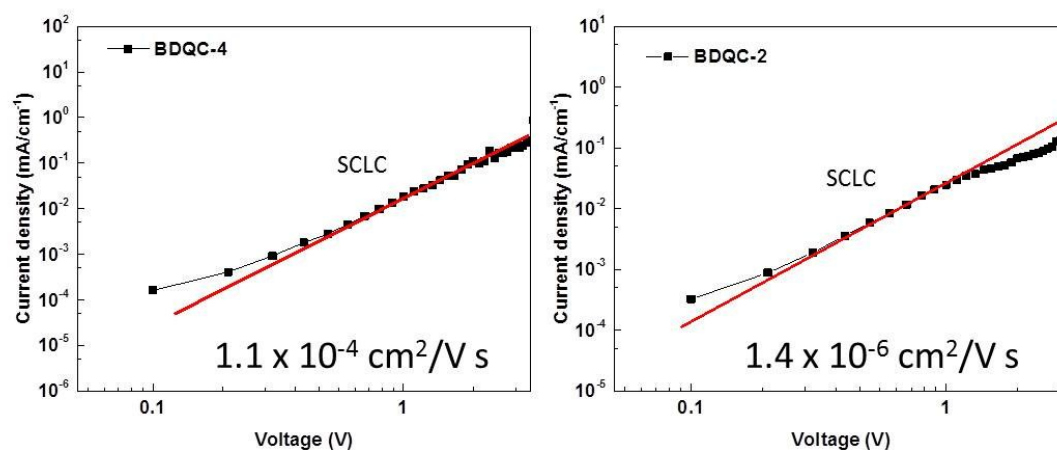


Figure S8. J-V curves measured in hole-only devices with the following architecture: ITO/NPD(10nm)/TCTA(10nm)/EML (50nm)/MoO₃ (10nm)/Al. The hole mobilities displayed in the inset were determined using the SCLC method.